On the Effects of Buoyancy Flux on Continental Shelf Circulation

LEONARD J. PIETRAFESA AND GERALD S. JANOWITZ

Department of Marine Science and Engineering, North Carolina State University, Raleigh 27650

(Manuscript received 6 December 1978, in final form 15 May 1979)

ABSTRACT

The effects of surface buoyancy flux, atmospheric wind stress and bottom topography on the horizontal and vertical structure of the density and alongshore velocity fields over a continental shelf are investigated within the context of a two-dimensional steady-state model. Using an iterative procedure, similarity solutions are obtained which include the important nonlinear advective effects in the density diffusion equation. In the absence of a wind stress, a reasonable value for the surface buoyancy flux produces alongshore velocities on the order of 20 cm s^{-1} and an upwelling-like vertical plane circulation. The depth variation across the shelf significantly affects the vertical structure of the density and velocity fields. The introduction of upwelling favorable winds decreases the horizontal density gradient and its associated baroclinic current. A simple physical explanation for this effect, based on heat conservation, is presented.

1. Introduction

The relative importance of the various air-sea transfers which influence the dynamics and mass field distribution on a continental shelf have not yet been fully established either by theory or field observations. It is generally acknowledged that the effects of mechanical surface wind forcing are dominant in the relatively shallow continental margin regions of the earth. Consequently, field programs and theoretical attempts aimed at deducing the physics of the continental shelves tend to overlook the fundamental influence of nonzero buoyancy flux at the free surface of the coastal zone. Buoyancy flux can be effected by either air-sea mass or heat exchange or by lateral coastal freshwater input, such as that due to riverine or estuarine sources.

There is one noteworthy exception to the apparent neglect of non-mechanical surface exchange forcing in the oceanographic literature: Stommel and Leetma (1972) discriminated between wind-driven and river runoff modes of shelf circulation by considering a hypothetical circulation on a flat, semi-infinite, vertically homogeneous continental shelf. Although Stommel and Leetma were able to estimate the shoreward distance of salt penetration from a specified shelf break salinity value, their neglect of horizontal mixing, topographic variation, and their imposition of a natural constraint that the top-to-bottom vertical integral of the horizontal mass flux equals zero, limit insights into the physics of the problem which is developed in this paper.

The nature of the vertical and horizontal structure of the oceanic density and alongshore velocity fields induced by surface buoyancy flux and a determination of how and why these fields vary with changes in the alongshore wind stress and bottom topography have not been addressed in the literature and are the subject of this work. In essence, the solutions presented here will demonstrate the interacting, mutual effects of both momentum and buoyancy sources at the surface.

2. Theoretical formulation

The steady-state circulation of a stratified, incompressible Boussinesq fluid rotating with constant angular velocity $f/2$ about the vertical on a variable depth continental shelf is assumed to be independent of the alongshore spatial variable. Nonlinear momentum effects and lateral momentum exchange are neglected, though Garvine (1971) and Hidaka (1954) suggest that a lateral frictional boundary layer should be included in continental shelf circulation considerations. The effects of the neglected nonlinear terms in the momentum equations will be considered after solutions have been obtained. Lateral mixing is included in the density equation, since Bowden (1965) showed that vertical turbulent mixing can, in the presence of a vertical gradient of velocity, yield an effective lateral diffusion of density. Additionally, the Froude number is assumed small and the system is assumed to be in hydrostatic balance. The system of equations is thus not unlike those used by Hsueh and Kenney (1972), Pietrafesa (1973) and Pedlosky (1974a, b), who independently investigated various aspects of shelf dynamics.

0022-3670/79/050911-08$06.00

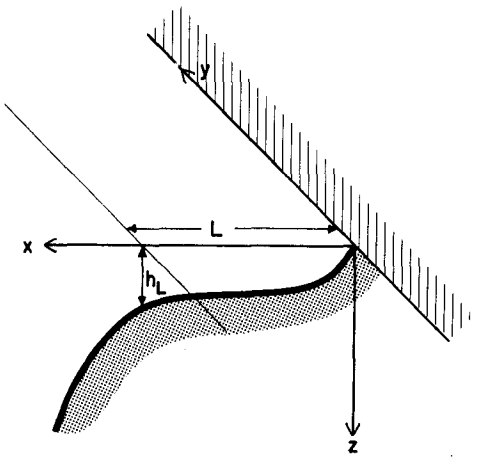

FIG. 1. Geometry of the problem.

Consider the flow over a shelf of width L and depth h in a right-handed Cartesian coordinate frame with x positive west, y positive north and z positive down (cf. Fig. 1) described by the equations

$$fv = -\frac{1}{\rho_0}P_x + (Au_z)_z, \tag{1}$$

$$-fu = (Av_z)_z, \tag{2}$$

$$P_z = g\rho, \tag{3}$$

$$u_x + w_z = 0, \tag{4}$$

$$u\rho_x + w\rho_z = (D\rho_x)_x + (K\rho_z)_z, \tag{5}$$

where subscripts denote partial differentiation; u, v and w are, respectively, velocity components in the x, y and z directions; P is the pressure, ρ the fluid density, g the gravitational acceleration, and A, K and D denote the vertical eddy viscosity, vertical eddy diffusion and horizontal eddy diffusion exchange coefficients, respectively.

To obtain governing equations for the velocity and density fields, we first introduce a streamfunction ψ such that

$$u = -\psi_z \quad \text{and} \quad w = \psi_x. \tag{6}$$

Relation (4) is then identically satisfied in terms of ψ.

The boundary conditions on the velocity field require that the exchange of momentum be continuous across the surface, that there be a rigid lid on the system, and that the velocity vanish at the bottom. The conditions on the velocity field are

$$\psi(0,x) = 0, \tag{7a}$$

$$A\psi_{zz}(0,x) = T^x(x), \tag{7b}$$

$$Av_z(0,x) = -T^y(x), \tag{7c}$$

$$\psi(h,x) = 0, \tag{7d}$$

$$\psi_z(h,x) = 0, \tag{7e}$$

$$v(h,x) = 0, \tag{7f}$$

where $T^x(x)$ and $T^y(x)$ are the x and y components, respectively, of the kinematic wind stress vector $\mathbf{T}$, i.e., τ/ρ. If we now introduce the streamfunction into (2) and integrate (2) with respect to z, we obtain

$$Av_z = f\psi + g(x). \tag{8}$$

Using the boundary condition (7c), we find that

$$v_z(x,z) = \frac{f\psi}{A}(x,z) - \frac{T^y}{A}(x). \tag{9}$$

We next assume A, K and D to be independent of z and integrate (9) in z, using condition (7f) to obtain

$$v = \frac{T^y}{A}(x)[h(x) - z] - \frac{f}{A}\int_z^{h(x)} \psi(x,z')dz'. \tag{10}$$

Hence, v has been obtained in terms of ψ, with all of the boundary conditions on v satisfied.

To obtain an equation for ψ we first differentiate (1) with respect to z, use (3) to eliminate P, and (9) to eliminate v, and introduce ψ using (6). The equation governing ψ is

$$\psi_{zzzz} + \frac{f^2}{A^2}\psi = \frac{-g\rho_x}{\rho_0 A} + \frac{f}{A^2}T^y \tag{11}$$

with the introduction of ψ into (5), the advective–diffusive density balance becomes

$$\psi_x\rho_z - \psi_z\rho_x = (D\rho_x)_x + K\rho_{zz}. \tag{12}$$

The boundary conditions on the nonlinearly coupled set (11) and (12) include not only (7a), (7b), (7d) and (7e) but also those of continuous exchange of buoyancy flux Q across the navifacial surface and of an insulated bottom, i.e.,

$$\rho_z(x,0) = Q(x)/K, \tag{13a}$$

$$K\rho_z(x,h) - h_x D\rho_x(x,h) = 0. \tag{13b}$$

Here Q represents the net freshwater addition to (or depletion from) the surface by mechanisms such as heating, cooling, evaporation or precipitation. While oceanic surface cooling is a problem of interest, it can lead to unstable vertical density profiles and will not be considered here.

The system of equations and boundary conditions now includes (11) and (12) which with (7a), (7b), (7d) and (7e) and (13a) and (13b) can be used to obtain ψ and ρ. The solution of v then becomes an auxiliary calculation as expressed in relation (10).

In the analysis which follows, several parameters which characterize the motion arise and are defined below. Note that the subscript L denotes the value of a parameter evaluated at the outer edge of the shelf ($x = L$).

$$\hat{\rho} = |Q_L|h_L/K_L$$

$$T_b = g\hat{\rho}A_L/\rho_0 Lf$$

$$T_m = \max\{[(T_L^y)^2 + (T_L^x)^2]^{1/2}, T_b\}$$

$$\Psi_L = T_m/f$$
$$V_L = T_m/fh_L$$
$$R_a = h_L{}^4 g\hat{\rho}/\rho_0 A_L \Psi_L L$$
$$\mathrm{E} = A_L/fh_L{}^2$$
$$\mathrm{RaE}^2 = g\hat{\rho}A_L/\rho_0 f^2 \Psi_L L = T_b/T_m \ (\leqslant 1)$$
$$\gamma = \Psi_L L/D_L h_L$$
$$\Gamma = K_L L^2/D_L h_L{}^2. \tag{14}$$

Here RaE^2 is a measure of the relative strengths of buoyancy effects to wind-induced advection in the momentum balance and γ is a measure of the effects of advection of the density field. T_m represents the maximum of the larger of either the square root of the sum of the squares of the horizontal wind stress components or of the quantity T_b, which will be referred to as the "buoyancy stress" and Γ represents the ratio of horizontal to vertical diffusive mixing time scales. We now proceed with the analysis. Ra is the Rayeigh number and E the Ekman number.

A separation transformation of Eqs. (11) and (12) will be performed with the introduction of a new set of variables such that

$$\zeta = \frac{x}{L} \tag{15a}$$
$$\eta = \frac{z}{h_L}\zeta^{\alpha} \tag{15b}$$
$$h = h_L \zeta^{-\alpha} \ (\alpha < 0) \tag{15c}$$
$$\psi = \psi_L \phi(\eta)\zeta^{\alpha_1} \tag{15d}$$
$$\rho(x,z) = \hat{\rho}[\theta(\eta)\zeta^{\alpha_2} - \theta(0)] + \rho(L,0) \tag{15e}$$
$$A = A_L \zeta^{\alpha_3} \tag{15f}$$
$$D = D_L \zeta^{\alpha_4} \tag{15g}$$
$$K = K_L \zeta^{\alpha_5} \tag{15h}$$
$$V = V_L \zeta^{\alpha_{10}/2}\left[T_L{}^y(1-\eta)/ET_m \right.$$
$$\left. ET_m - \int_{\eta}^{1} \phi d\eta'/\mathrm{E}\right] \tag{15i}$$
$$T^x(x) = T_L^x \zeta^{\alpha_8} \tag{15j}$$
$$T^y(x) = T_L^y \zeta^{\alpha_9} \tag{15k}$$
$$Q(x) = Q_L \zeta^{\alpha_{10}}. \tag{15l}$$

Note that at $z = 0$, $\eta = 0$ and at $z = h$, $\eta = 1$ for all values of x.

Substituting these transformed variables into equations (7), (11), (12) and (13) and separating out the explicit x dependences then yields the following set of ordinary differential equations:

$$\Phi_{\eta\eta\eta\eta} + E^{-2}\Phi = -\mathrm{Ra}(\alpha_2\theta + \alpha\eta\theta_\eta) + T_L^y/T_m E^2, \tag{16}$$

$$(\Gamma + \alpha^2\eta^2)\theta_{\eta\eta} + [\alpha\eta(3\alpha_2 - 1) - \gamma(\alpha_2 - 2\alpha - 1)\Phi]\theta_\eta + [\alpha_2(\alpha_2 - \alpha - 1) + \gamma\alpha_2\Phi_\eta]\theta = 0 \tag{17}$$

and boundary conditions

$$\phi(0) = 0, \tag{18a}$$
$$\phi_{\eta\eta}(0) = T_L^x/T_m \mathrm{E}, \tag{18b}$$
$$\phi_\eta(1) = 0, \tag{18c}$$
$$\phi(1) = 0, \tag{18d}$$
$$\theta_\eta(0) = \pm 1 \ (+ \text{ for heating}, - \text{ for cooling}), \tag{18e}$$
$$(\Gamma + \alpha^2)\theta_\eta(1) + \alpha\alpha_2\theta(1) = 0. \tag{18f}$$

The similarity conditions are

$$\left.\begin{aligned} \alpha_1 &= \alpha_8 = \alpha_9 = \tfrac{1}{2}(\alpha_{10} - 2\alpha) \\ \alpha_2 &= 1 + \alpha + \alpha_{10}/2 \\ \alpha_3 &= -2\alpha \\ \alpha_4 &= 1 + \alpha_{10}/2 \\ \alpha_5 &= (\alpha_{10} - 4\alpha - 1)/2 \end{aligned}\right\}. \tag{19}$$

Thus, the structure of the dependent variables ψ, ρ and v in the x direction (α_1, α_2 and α_{10}, respectively), as well as the required attenuation of the eddy coefficients (α_3, α_4 and α_5) and the wind stresses (α_8 and α_9), are directly related to the power law of the bottom (α) and the surface buoyancy flux functional structure (α_{10}). The eddy coefficients are treated as functions of x only, simply as a matter of mathematical convenience and because the intent of this paper is to indicate the importance of the buoyancy flux "stress."

Eqs. (16) and (17) are separately linear in either dependent variable but are nonlinearly coupled in the variables ψ and ρ when either is expressed in terms of the other. The nature of this coupling suggests that a straightforward solution may not be possible. It is of note that, in general, $\mathrm{E} \ll 1$, so that a boundary-layer technique of the following iterative scheme could be used in an attempt to obtain solutions to the system (see the Appendix). Further, for $\mathrm{E} \ll 1$, outside of the Ekman layers, (16) indicates that RaE^2 is the measure of the effect of ρ_x on ψ.

We will now solve the coupled set (16) and (17), using a simultaneous iterative technique. We first rewrite Eqs. (16) and (17) operationally as

$$L_1(\phi) = \mathrm{RaE}^2 L_2(\theta) \tag{16a}$$

and

$$L_3(\phi,\theta,\gamma) = 0, \tag{17a}$$

where L_1, L_2 and L_3 denote appropriate differential operators. Then for the iterative approach, we rewrite these equations as

$$L_1(\phi_m) = \mathrm{RaE}^2(L_2\theta_{m-1}), \tag{20}$$
$$L_3(\phi_m,\theta_m) = 0, \tag{21}$$

where $m = 1, 2, 3, \ldots$. Next we let $\theta_0 = 0$ and solve (20) for ϕ_1, subject to conditions (18a)–(18d).

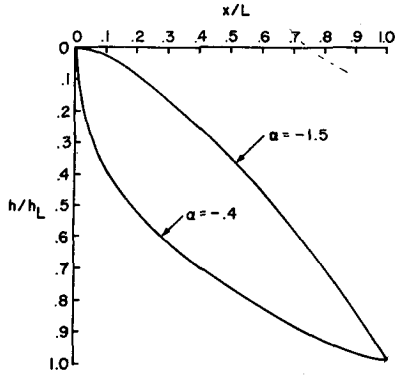

FIG. 2. Deep ($\alpha = -0.4$) and shallow ($\alpha = -1.5$) bottom topographies.

We then solve for θ_1 from (21), which becomes a linear equation with nonconstant coefficients, subject to conditions (18e) and (18f). With θ_1 thus determined, ϕ_2 is found from (20) and then θ_2 from (21). We continue iterating and superposing partial solutions, in the manner described, until two consecutive solutions for ϕ and θ agree to, at least, four significant figures. For wind-driven cases, with $\gamma = 1.0$ and $\mathrm{RaE}^2 \leq 0.5$, 10–15 iterations were required for solution convergence in both ϕ and θ. For strictly buoyancy driven cases, that is, wind forcing set to zero, with $\mathrm{RaE}^2 = 1.0$ but $\gamma \leq 0.2$, approximately five iterations were necessary for solution convergence. We note that since the homogeneous solutions of (20) are known, the particular solution for ϕ was explicitly determined by the variation of parameters technique; a Runge-Kutta scheme was used for (21).

3. Numerical results

In the cases to be discussed, principal emphasis will be on those flows driven by surface buoyancy flux. Such flows have been relatively neglected in the literature. Additionally, cases which include both mechanical and thermal surface forcing will be discussed. Two different bottom topographies, including that of a deep inner shelf, $\alpha = -0.4$ and of a shallow inner shelf $\alpha = -1.5$, are considered. Fig. 2 depicts the topographies used; the nomenclature is obvious.

The cases to be discussed are broken into two categories: the first four cases concern the purely buoyancy flux-driven modes of circulation and density distribution; the last three cases have, in addition to a surface buoyancy flux, a negative (upwelling favorable) alongshore wind stress of three different magnitudes. The parameter values used in the various cases are presented in Tables 1 and 2. The surface heat flux magnitude, Q_L, used in the study corresponds to an input of heat into the ocean of 150 cal cm^{-2} day^{-1} with a coefficient of thermal expansion of 3.45(10-4) $^\circ\mathrm{C}^{-1}$.

In Figs. 3 and 4, we present the density $\rho(L,\eta) - \rho(L,0)$, and longshore velocity $v(L,\eta)$ profiles for Case 1, the weakly advective, and Case 2, the purely diffusive, deep shelf ($\alpha = -0.4$) buoyancy flux-forced flows. The results indicate that for our assumption of uniform surface heating ($\alpha_{10} = 0$), the shallower coastal waters become warmer than the offshore waters and hence the offshore surface density gradient ρ_x is positive; alternatively one could say that since heat is being added at the surface it must diffuse through the seaward boundary and the offshore surface temperature gradient must be negative and ρ_x must be positive. With $\rho_x > 0$, the longshore velocity will increase upward starting from the zero no-slip condition at the bottom. Hence, the primary effect of the heating is to drive a longshore flow in the positive y direction. Since the primary longshore flow has $v_z < 0$ (z positive downward) at the surface, an upper Ekman layer must develop to bring v_z to zero there; this layer can be considered similar to one induced by a wind stress in the negative y direction, i.e., an upwelling favorable wind stress. Thus, we have an offshore flow near the top and an onshore flow at the bottom. This vertical plane circulation then acts in two ways on the density field. First, since fluid parcels move rapidly offshore and onshore near the surface and bottom boundaries, respectively, the diffusive time scales are sufficiently long so that diffusion cannot act to change the density of a parcel as much as for $\gamma = 0$ and, thus ρ_x at the surface is diminished somewhat by the vertical plane circulation over a purely diffusive picture. Alternatively, with the net heat input at the top fixed, warm surface waters flow offshore carrying some heat off the shelf which means that less heat is required to be diffused across the seaward vertical boundary to relieve the system of excess heat and thus the surface value of ρ_x is diminished, at $x = L$, in Case 1, the weakly advective, case, relative to Case 2, the purely diffusive case. Second, the upper layer brings warm coastal waters offshore and the lower layer brings cool waters onshore. The surface (bottom) layer acts as a heat source (sink) for the rest of the water column; thus, we see an increase in the vertical variation of density due to the vertical plane circulation.

TABLE 1. List of parameters common to all cases.

$L = 50$ km	$\mathrm{E} = 2.5 \times 10^{-3}$
$h_L = 200$ m	$\hat{\rho} = 5.5 \times 10^{-4}$ g cm^{-3}
$A_L = 100$ cm^2 s^{-1}	$T_L^* = 0$
$D_L = 1.38 \times 10^6$ cm^2 s^{-1}	$T_b = 0.11$ cm^2 s^{-2}
$K_L = 22$ cm^2 s^{-1}	$\Gamma = 1.0$
$Q_L = 150$ cal cm^{-2} day^{-1}	$\alpha_{10} = 0$
$f = 10^{-4}$ s^{-1}	

TABLE 2. List of parameters which vary from case to case.

Case no.	T^y_L (cm^2 s^{-2})	T_m (cm^2 s^{-2})	Ψ_L (cm^3 s^{-1})	V_L (cm s^{-1})	γ	RaE^2	α
1	0	$1.1(10^{-1})$	$1.1(10^3)$	$5.5(10^{-2})$	$2(10^{-1})$	1.0	$-4(10^{-1})$
2	0	$1.1(10^{-1})$	$1.1(10^3)$	$5.5(10^{-2})$	0.0	1.0	$-4(10^{-1})$
3	0	$1.1(10^{-1})$	$1.1(10^3)$	$5.5(10^{-2})$	$2(10^{-1})$	1.0	-1.5
4	0	$1.1(10^{-1})$	$1.1(10^3)$	$5.5(10^{-2})$	0.0	1.0	-1.5
5	$1.1(10^{-1})$	$1.1(10^{-1})$	$1.1(10^3)$	$5.5(10^{-2})$	$2(10^{-1})$	1.0	$-4(10^{-1})$
6	$3.85(10^{-1})$	$3.85(10^{-1})$	$3.85(10^3)$	$1.93(10^{-1})$	$7(10^{-1})$	0.286	$-4(10^{-1})$
7	$4.4(10^{-1})$	$4.4(10^{-1})$	$4.4(10^3)$	$2.2(10^{-1})$	$8(10^{-1})$	0.25	$-4(10^{-1})$

For $\gamma = 0$, the purely diffusive density balance, $\rho_x(L,0) = 0.97 \times 10^{-10}$ g cm^{-4} and for $\gamma = 0.2$, the weakly advective density balance, $\rho_x(L,0) = 0.81 \times 10^{-10}$ g cm^{-4}.

We next consider the shallow shelf ($\alpha = -1.5$) Cases 3 and 4 presented in Tables 1 and 2. The results for the density and longshore velocities are given in Figs. 5 and 6 for $\gamma = 0$ and 0.2. Since the vertical extent of the water columns for $x < L$ are less in these two cases than for the deep shelf case, one would expect larger values of surface ρ_x and, indeed, $\rho_x(L,0) = 2.09 \times 10^{-10}$ g cm^{-4} for $\gamma = 0$, and $\rho_x(L,0) = 1.97 \times 10^{-10}$ g cm^{-4} for $\gamma = 0.2$; more than twice the deep shelf values. However, by comparing the longshore velocity profiles for the deep (Fig. 4) and shallow shelf (Fig. 6) cases, we see that away from the upper surface ρ_x is actually less for the shallow than for the deep shelf case. This is so because as we move offshore at constant depth (z), we move relatively higher in the water column in the shallow than in the deep shelf case as is obvious from the relationship $\partial\eta/\partial x = \alpha\eta/x$.

The combined effects of uniform heating and negative atmosphere wind stress $T^y = T^y_L\xi^{0.4}$ are now investigated for the deep shelf case. In Fig. 7 the longshore velocity profiles are presented for Cases 5, 6, 7 and for comparative purposes Case 1.

In the absence of baroclinic effects, with RaE^2 = 0, for an upwelling favorable wind, we expect an offshore flowing top Ekman layer, an onshore flowing bottom Ekman layer and an interior longshore velocity in the negative y direction of speed $-(2)^{1/2}T^y_L/fh_L\mathrm{E}^{1/2}$. The surface alongshore velocity is negative and of speed $-3T^y_L/2^{1/2}fh_L\mathrm{E}^{1/2}$. Introducing the baroclinic pressure gradient and combining the barotropic and baroclinic alongshore flows as shown in Fig. 7 yields the following picture. Just above the bottom layer a negative alongshore velocity is generated since the bottom Ekman layer must transport fluid toward the coast. As we move upward in the water column baroclinic effects are realized and the alongshore velocity becomes less negative. When we enter the upper Ekman layer the velocity becomes somewhat more negative. The wind affects the density field such that as the effective surface stress increases, the offshore surface flow magnitude increases, the time to cross the shelf in the top Ekman layer is diminished and, as diffusion has less time to act on a fluid parcel, its change in density and hence ρ_x decrease. Alternatively, the heat leaving in the top Ekman layer increases with $|T^y_L|$ which requires that less heat be diffused out through the vertical seaward boundary. Hence the surface offshore temperature and density gradients at $x = L$ decrease in magnitude. For $\rho T^y_L = 0.0$, -0.11, -0.385 and -0.44 dyn cm^{-2},

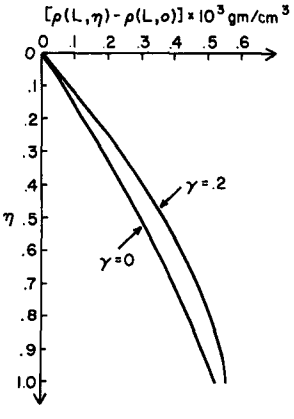

FIG. 3. Deep shelf density profile.

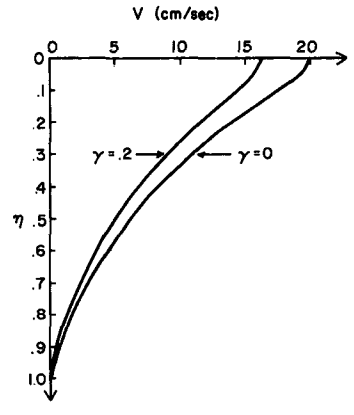

FIG. 4. Deep shelf alongshore velocity profile.

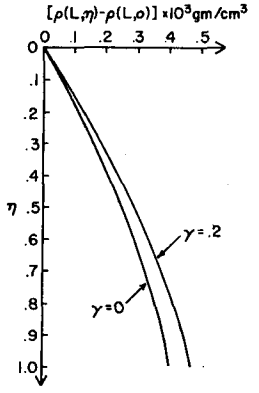

FIG. 5. Shallow shelf density profile.

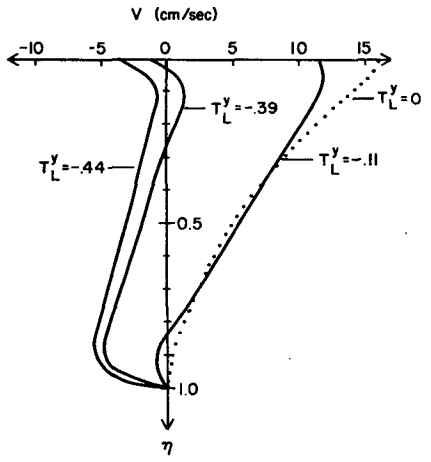

FIG. 7. Alongshore velocity profiles for (kinematic) upwelling favorable wind stresses; $T_L^y = -0.11$, -0.39 and -0.44 cm^2 s^{-2}.

the corresponding values of $\rho_x(L,0)$ are (cf. Fig. 8) $8.1(10^{-11})$, $6.3(10^{-11})$, $2.2(10^{-11})$ and $1.6(10^{-11})$ g cm^{-4}. The baroclinic effect on the longshore velocity is clearly inversely proportional to the wind stress magnitude. Stommel and Leetma (1972) note the same effect of T_L^y on ρ_x; however, since their model neglects horizontal mixing and their density field is depth independent of z to lowest order, the explanation given here cannot apply to their results which are a consequence of enhanced advection. As indicated earlier, the Ekman layers also act as sources and sinks of heat thereby affecting the interior vertical density structure. The change in the vertical buoyancy flux ($K\rho_z$) across the Ekman layer is proportional to $M_{ex}\rho_x$, where M_{ex} is the net Ekman layer flux. As the wind increases, M_{ex} increases but ρ_x decreases and the capacity for the Ekman layer to change the vertical heat flux stabilizes. For the purely diffusive density field $[\rho(L,h_L) - \rho(L,0)] = 0.4(10^{-4})$ g cm^{-3}. For the case of heating alone and $\gamma = 0.2$, this value is increased by some twenty percent to 0.47×10^{-3} g cm^{-3}. For $\rho T_L^y = -0.11$, -0.385 and -0.44 dyn cm^{-2} this value is 0.51×10^{-3}, 0.51×10^{-3} and 0.50×10^{-3} g cm^{-3}. Thus the capacity of the wind to change the vertical variation of density is limited, at least for moderate winds. An important effect of the wind on the longshore velocity is to weaken the baroclinic component.

This model neglects nonlinear and horizontal turbulent mixing effects in the momentum equations. As long as $v_x/f \ll 1$ (which is well satisfied for the cases presented) and $A_H \ll 10^8$ cm^2 s^{-1} these effects are unimportant. The similarity solution imposes many restraints on the system but it does allow for the inclusion of advective terms in the density equation, which have been shown to be of extreme importance. Further, even modest values of buoyancy flux produce reasonable values for alongshore velocities.

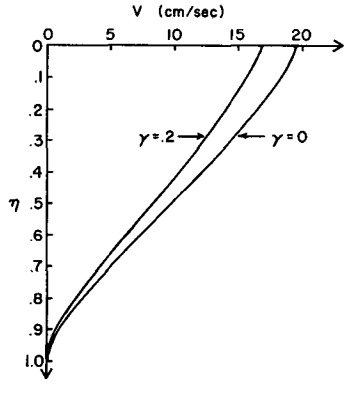

FIG. 6. Shallow shelf alongshore velocity profile.

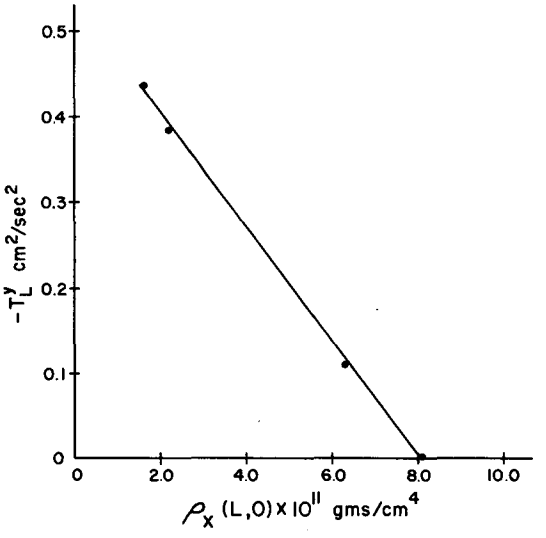

FIG. 8. Horizontal density gradient at $\eta = 0$ as a function of upwelling favorable wind stresses: $T_L^y = 0.0$, -0.11, -0.39 and -0.44 cm^2 s^{-2}.

4. Conclusions

We have examined the effects of surface buoyancy flux, alongshore wind stress, and bottom topography on the structure of the density and velocity fields of the two-dimensional steady flow over a continental shelf. We have found that surface buoyancy flux acting alone can force an upwelling type of circulation and alongshore speeds on the order of 20 cm s^{-1}. Deeper shelves have been found to have a greater vertical density variation and weaker deep alongshore currents than do shallower shelves. Due to the surface buoyancy flux-induced vertical variation in density, that is, relatively warm surface as compared to bottom waters when upwelling favorable winds are introduced, the additional loss of heat caused by the augmented offshore upper Ekman flux of these relatively warm waters requires that less heat be diffused across the seaward boundary of the region to balance a fixed heat input at the surface. Thus, upwelling favorable winds decrease the horizontal density gradient and the associated baroclinic current relative to the strictly buoyancy flux-driven case. For moderate winds the alongshore flow below the top Ekman layer may be counter to the wind, a situation which is observed in the data and which may demonstrate the importance of surface buoyancy flux.

Acknowledgments. The authors gratefully acknowledge support for this work by the Department of Energy under Contract EY-76-S-09-0902.

APPENDIX

Boundary Layer Analysis

If the Ekman number E is small compared to one with RaE^2 and $\gamma = O(1)$, we can use a boundary-layer technique to obtain a second-order, nonlinear, governing equation and boundary conditions on θ with errors of order $E^{1/2}$. With θ determined, ϕ and v follow in a straightforward manner.

First we define interior solutions for ϕ and θ, say, ϕ_i and θ_i. These solutions are O(1), have $\partial T/\partial\eta = O(1)$, exist over the interval $0 \leq \eta \leq 1$, and satisfy the equations

$$\phi_i = T_L^{\eta} T_m - \mathrm{RaE}^2(\alpha_2\theta_i + \alpha\eta\theta_{i\eta}), \quad \text{(A1)}$$

$$(\Gamma + \alpha^2\eta^2)\theta_{i\eta\eta} + (\alpha\eta(3\alpha_2 - 1) - \alpha(\alpha_2 - 2\alpha - 1)\phi_i)\theta_{i\eta} + (\alpha_2(\alpha_2 - \alpha - 1) + \gamma\alpha_2\theta_{i\eta})\theta_i = 0. \quad \text{(A2)}$$

Inserting (A1) into (A2) yields a single second-order nonlinear governing equation for θ_i. With appropriate boundary conditions on θ_i, (A2) and then (A1) can be solved. To obtain these boundary conditions, we must examine the boundary-layer corrections to θ and ϕ, say, $\tilde{\theta}$ and $\tilde{\phi}$. The boundary-layer corrections vanish away from $\eta = 0$, 1 and near the boundaries $\phi = \phi_i + \tilde{\phi}$ and $\theta = \theta_i + \tilde{\theta}$. The boundary-layer corrections have the properties

$$\tilde{\phi} = O(1), \quad \frac{\partial}{\partial\eta} = O(E^{-1/2}),$$

$$\tilde{\theta} = O(E^{1/2}), \quad \frac{\partial\tilde{\theta}}{\partial\eta} = O(1).$$

The equations governing $\tilde{\phi}$ and $\tilde{\theta}$ near the top are

$$E^2\tilde{\phi}_{\eta\eta\eta\eta} + \tilde{\phi} = 0 + O[(RaE^2)E^{1/2}], \quad \text{(A3)}$$

$$E^{1/2}[\Gamma\tilde{\theta}_{\eta\eta} + \gamma\alpha_2\tilde{\phi}_\eta\theta_i(0)] = 0 + O(E^{1/2}). \quad \text{(A4)}$$

The equations governing $\tilde{\phi}$ and $\tilde{\theta}$ near the bottom are

$$E^2\tilde{\phi}_{\eta\eta\eta\eta} + \tilde{\phi} = -RaE^2\alpha\tilde{\theta}_\eta + O[(RaE^2)E^{1/2}], \quad \text{(A5)}$$

$$E^{1/2}[(\Gamma + \alpha^2)\tilde{\theta}_{\eta\eta} + \gamma\alpha_2\tilde{\phi}_\eta\theta_i(1)] = 0 + O(E^{1/2}). \quad \text{(A6)}$$

The boundary conditions at the top are

$$\tilde{\phi}(0) + \phi_i(0) = 0, \quad \text{(A7)}$$

$$E\tilde{\phi}_{\eta\eta}(0) = T_L^x/T_m + O(E), \quad \text{(A8)}$$

$$\tilde{\theta}_\eta(0) + \theta_\eta(0) = 1. \quad \text{(A9)}$$

The boundary conditions at the bottom are

$$\tilde{\phi}(1) + \phi_i(1) = 0, \quad \text{(A10)}$$

$$\tilde{\phi}_\eta(1) = 0 + O(E^{1/2}), \quad \text{(A11)}$$

$$(\Gamma + \alpha^2)[\tilde{\theta}_\eta(1) + \theta_\eta(1)] = \alpha\alpha_2\theta_i(1) + O(E^{1/2}). \quad \text{(A12)}$$

To obtain these conditions we used the requirements that

$$\tilde{\theta} = O(E^{1/2}), \quad \phi_{i\eta}/\tilde{\phi}_\eta = O(E^{1/2})$$

and

$$\phi_{i\eta\eta}/\phi_{\eta\eta} = O(E).$$

Eqs. (A4) and (A6) may be integrated with respect to η under the conditions that $\tilde{\phi}$ and $\tilde{\theta}$ vanish away from the boundary to obtain, near the top,

$$\Gamma\tilde{\theta}_\eta + \gamma\alpha_2\tilde{\phi}\theta(1) = 0, \quad \text{(A13)}$$

and near the bottom

$$(\Gamma + \alpha^2)\tilde{\theta}_\eta + \gamma\alpha_2\tilde{\phi}\theta i(1) = 0. \quad \text{(A14)}$$

We now evaluate these last two equations at $\eta = 0$ and $\eta = 1$ respectively and use (A1), (A7) and (A10) to obtain

$$\tilde{\theta}_\eta(0) = \frac{\gamma}{\Gamma}\alpha_2\theta_i(0)\left\{\frac{T_L^{\eta}}{T_m} - \mathrm{RaE}^2\alpha_2\theta_i\big|_{\eta=0}\right\}, \quad \text{(A15)}$$

$$\tilde{\theta}_\eta(1) = \frac{\gamma}{\Gamma + \alpha^2}\,\alpha_2\theta_i(1)\left\{\frac{T_\ell^y}{T_m} - \mathrm{RaE}^2(\alpha_2\theta_i + \theta_{i\eta})\big|_{\eta=1}\right\}. \tag{A16}$$

We now use these last two equations in (A9) and (A12) to obtain the boundary conditions on θ_i

$$\theta_{i\eta}(0) = 1 - \frac{\gamma}{\Gamma}\,\alpha_2\theta_i(0)\left\{\frac{T_\ell^y}{T_m} - \mathrm{RaE}^2\alpha_2\theta_i(0)\right\}, \tag{A17}$$

$$(\Gamma + \alpha^2)\theta_{i\eta}(1) = -\alpha\alpha_2\theta_i(1) - \gamma\alpha_2\theta_i(1)\left\{\frac{T_\ell^y}{T_m} - \mathrm{RaE}^2\alpha_2[\theta i(1) + \alpha\theta i_\eta(1)]\right\}. \tag{A18}$$

With expressions for $\phi_i(\eta)$ and $\phi_{i\eta}(\eta)$ evaluated from (A1) and substituted into (A2) the following nonlinear equation for θ_i results:

$$[\Gamma + \alpha^2\eta^2 - \gamma\alpha\alpha_2\,\mathrm{RaE}^2\eta\theta_i]\theta_{i\eta\eta} + \left[\alpha\eta(3\alpha_2 - 1) - \gamma(\alpha_2 - 2_\alpha - 1)\frac{T_\ell^y}{T_m} - \gamma\alpha_2(3\alpha + 1)\,\mathrm{RaE}^2\theta_i - \gamma(2_\alpha - 2\alpha - 1)\,\mathrm{RaE}^2\alpha\eta\theta_{i\eta}\right]\theta_{i\eta} + \alpha_2(\alpha_2 - \alpha - 1)\theta_i = 0. \tag{A19}$$

Eqs. (A17)–(A19) could be solved iteratively by first neglecting the θ_i terms in the brackets in (A19) and obtaining a solution, say θ_{i0}, subject to (A17) and (A18). Using θ_{i0} in (A19) we could generate θ_{i1}, etc. Since the coefficients of the θ terms in the brackets are generally small compared to the other terms in the brackets a few iterations would suffice and $\theta_i(\eta)$ could be determined. With θ_i determined $\tilde{\phi}$ could be easily determined subject to (A7), (A8), (A10) and (A11). We note that the governing equation for the bottom boundary layer becomes using (A14)

$$\mathrm{E}^2\tilde{\phi}_{\eta\eta\eta\eta} + \tilde{\phi}\left\{1 - \frac{\gamma\alpha\alpha_2\,\mathrm{RaE}^2\theta_i(1)}{\Gamma + \alpha^2}\right\} = 0.$$

Thus, the density field can effect the thickness of the bottom layer although this effect is quite small. For the deep shelf case previously discussed

$$-\gamma\alpha\alpha_2\,\mathrm{RaE}^2/(\Gamma + \alpha^2) = 0.0413,$$

$$\theta_i(1) = \mathrm{O}(1).$$

The heating (cooling) effect of the upper (lower) Ekman layer flux on θ_i can be seen from (A17) and (A18). If $T_\ell^y/T_m < 0$ (upwelling favorable wind), and $\alpha_2\theta_1(0)$, $\alpha_2\theta_1(1) > \mathrm{O}(\rho_x > 0)$ then $\theta_{1\eta}(0) > 1$ and $\theta_{i\eta}(1) > 0$.

We note here that the system of equations considered here is identical to that considered by Pietrafesa (1973) though the boundary conditions differ; he used a bilinear form of an expansion parameter based on the Shohat (1944) renormalization technique. The range of validity of the results was established by Struble and Pietrafesa (1978).

REFERENCES

Bowden, K., 1965: Horizontal mixing in the sea due to a shearing current. *J. Fluid Mech.*, **21**, 83–95.

Garvine, R. W., 1971: A simple model of coastal upwelling dynamics. *J. Phys. Oceanogr.*, **1**, 169–179.

Hidaka, K., 1954: A contribution to the theory of upwelling and coastal currents. *Trans. Amer. Geophys. Union*, **35**, 431–444.

Hsueh, Y., and R. N. Kenney, 1972: Steady coastal upwelling in a continuously stratified ocean. *J. Phys. Oceanogr.*, **2**, 27–33.

Pedlosky, J., 1974a: On coastal jets and upwelling in bounded basins. *J. Phys. Oceanogr.*, **4**, 3–18.

——, 1974b: Longshore currents, upwelling and bottom topography. *J. Phys. Oceanogr.*, **4**, 214–226.

Pietrafesa, L. J., 1973: Steady baroclinic circulation on a continental shelf. Ph.D. dissertation of Oceanography and Geophysical Group, University of Washington, 192 pp.

Shohat, J., 1944: On Van der Pol's and related non-linear differential equations. *J. Appl. Math.*, **15**, 568–574.

Stommel, H. M., and A. Leetma, 1972: Circulation on the continental shelf. *Proc. Nat. Acad. Sci.*, **69**, 3380–3384.

Struble, R. A., and L. J. Pietrafesa, 1978: Revised Euler-Shohat pertubation expansion. Dept. of Marine Science and Engineering Rep. No. 78-9, North Carolina State University, 23 pp.